

Passive harmonic mode-locking in soliton fibre lasers

A. B. Grudinin and S. Gray

Optoelectronics Research Centre, Southampton University
Southampton SO17 1BJ, UK

Abstract

We present an experimental and theoretical study of passively mode-locked fibre soliton lasers. Our theoretical analysis based on perturbation theory describes the soliton interactions which occur when pulse bunches form. Our results indicate that the non-soliton component emitted by the propagating solitons causes small changes of the central frequency of individual solitons and the strength and sign of this interaction between the soliton and dispersive waves depends on their mutual phase as well as on the soliton position within the soliton bunch. For a certain phase difference between the solitons and non-soliton component the interaction force becomes repulsive for all solitons within a soliton bunch and results in an almost uniform distribution of the pulses inside the laser cavity. The pulses are then locked in their temporal positions by acoustic effects.

We also demonstrate that the laser performance could be further improved by the use of a MQW saturable absorber in combination with the nonlinear amplifying loop mirror. In this instance the MQW sample acts not only as a fast saturable absorber but also as a passive phase modulator. We experimentally demonstrate that such a laser is capable of generating 500 fs pulses at repetition rates exceeding 2 GHz.

I. Introduction

Erbium doped fibres are almost ideal as the basic component for lasers and amplifiers operating near 1550 nm which is the wavelength of lowest fibre loss and where the combined effect of negative group velocity dispersion and Kerr nonlinearity gives rise to the possibility of generating optical solitons. That is why fibre lasers capable of producing of ultra-short nonlinear optical pulses have been the subject of considerable interest over the past several years.

There are two approaches in the development of short pulse fibre lasers. The first method is a traditional one and comes from "classical" laser physics and is based on the incorporation of an amplitude or phase modulator in the laser cavity in order to achieve mode-locking. The second method is based on the use of passive mode-locking techniques. The fundamental idea of passive mode-locking is to provide additional loss for the low-intensity radiation by incorporating of intensity-dependent component into the laser cavity.

Two main types of passively mode-locked lasers have been demonstrated. The first type exploits the Kerr nonlinearity of optical fibres [1-13] while the second one is based on multi-quantum well (MQW) semiconductor structures acting as fast saturable absorbers [14-18].

Historically the first example of a passively mode-locked fibre laser was the so-called figure of eight laser [1-3] which uses the nonlinear switching characteristics of a nonlinear amplifying loop mirror (NALM) to achieve mode-locking. The simplest type of passively mode-locked fibre lasers is a ring

configuration [5-10] where the effect of cross-phase modulation between orthogonally polarized eigen-modes results in a different state of polarization for low- and high-intensity components and the incorporation of a polarizer into the laser cavity causes the required loss difference to suppress low-level radiation and to achieve mode-locking. The similar idea has been also exploited in linear configuration [4,11-13].

Mode-locking based on fibre nonlinearity in combination with negative dispersion results in the generation of optical solitons i.e. transform-limited pulses with a strong relationship between the temporal width of the pulse and its energy. The pulsewidth is defined by the laser cavity parameters (primarily by the length and intracavity dispersion) and this leads to the fundamental difference between conventional mode-locked lasers and soliton lasers: a change in the pump power of a conventional laser results in a modification of the parameters of the generated pulses (peak intensity, pulsewidth etc) but any alterations in the pump power of soliton lasers changes the number of propagating pulses leaving the parameters of the individual pulses largely unchanged.

This remarkable feature of the soliton laser is the result of the specific output characteristics of fibre soliton lasers: the output radiation consists of a number of soliton pulses and a nonsoliton component. The number of circulating pulses is defined by the ratio of the stored intracavity energy to the soliton energy. Generally this ratio is not an integer and this results in the formation of the non-soliton component which plays the role of a buffer:

any excess of stored intracavity energy (caused for example by small fluctuations of pump power) translates into the nonsoliton component. The energy quantization effect [5] of FSLs results in excellent stability of the duration and energy of the individual pulses, but also leads to pulse repetition rate instabilities which for many applications is unacceptable. One solution is to operate the laser with just a single pulse inside the cavity but this generally leads to low repetition rates (~ 5 MHz) and correspondingly low output power unless short cavities of a few metres length are used [19-21]. Other techniques involving additional sub-cavities [22], extra-cavity feedback [23] or intracavity modulation [24] have been demonstrated, enabling higher harmonic mode-locking and higher output powers to be obtained; however, these techniques would appear to be difficult to implement in practical systems.

The purpose of this paper is to analyse and identify the main effects affecting soliton dynamics inside the passively mode-locked fibre cavity with the aim to provide a guide for the design and optimization of passively mode-locked fibre lasers operating in the GHz regime.

II. Femtosecond fiber ring lasers.

2.1 Experimental configuration and results

The laser configuration is shown in Fig.1 and is similar to that described elsewhere [9]. The laser cavity comprises 4 m of Er/Yb codoped fibre, a length of standard telecom fibre (chromatic dispersion $D = 17$ ps/nm · km at 1550 nm), a polarization dependent isolator and two sets of polarization controllers

to set the appropriate state of polarization required for self-starting mode-locking. Typically with 500 mW of pump power from a conventional source operating at 1064 nm we obtained 35-50 mW of laser output power. At such pump powers the mode-locking self-starts at practically any position of polarization controllers PC2 provided PC1 is suitably set. To reduce pump power amplitude noise an external feedback circuit was used that kept pump power fluctuations to below 1%.

The laser pulsewidth depends on the cavity length and dispersion and for 60 m length it was 1.4 ps. Fig.2 shows a typical laser spectrum indicating the presense of a non-soliton component in the form of a frequency-shifted narrow-band peak. As we show below, this non-soliton component plays significant role in the laser capability to operate in a harmonically mode-locked regime. The point of the "second threshold " or "mode-locking threshold" corresponds to an output power of several milliwatts and the energy quantization effect results in formation of some 100 pulses running inside the cavity.

The most common regime of operation of a passively mode-locked soliton fibre laser is with an ill-defined repetition frequency with sometimes complicated pulse motion as described in [4]. However at certain positions of the PCs the laser produced "tightly bunched" pulses. If the position of PC1 is then suitably adjusted (leaving the position of PC2 is unaltered) the pulse bunch breaks up into a stable temporal pattern. The transformation from the bunched pulse regime to the stable harmonic pattern occures over a period

of several seconds with respect to the change in position of PC1. Observing the dynamics of the process on an oscilloscope this transient regime is characterised by a temporal stretching of the original pulse bunches at a speed of 10ns/s (or 2 m/s in conventional units) until the whole time domain is occupied. This is then followed by a gradual rearrangement of pulse separation until a stable harmonic pulse train is formed. The laser repetition rate can be easily changed by changing the pump power (and hence intracavity energy).

One of the most important characteristics of harmonically mode-locked lasers is time jitter. The time jitter can be measured by analysis of the rf spectrum of the laser output intensity [25]. Generally this spectrum consists of a main peak sitting on a broad pedestal. Knowing the intensity and bandwidth of the pedestal one can deduce the time jitter of the laser. Fig.3 shows the time jitter dependence as a function of the repetition rate frequency for a laser cavity fundamental frequency of 5.8 MHz and pulsewidth of 0.8 ps. The graph shows a strong oscillatory behaviour and a general tendency for the jitter to decrease at frequencies around 500 MHz. The lowest jitter of 1.1 ps (100 - 550 Hz) was observed at the frequency of 526 MHz. A similar oscillatory dependence (with maxima at the same frequencies) was observed when the pump power feedback loop was switched off, but the lowest time jitter was then around 10 ps. Note also that the same general behaviour was also observed for several other different cavity lengths.

By changing the length of the laser cavity we were able to study the jitter

for different pulsewidths and noticed that the shorter the pulses the lower was the time jitter. The lowest jitter of 600 fs (100 -550 Hz) was obtained for 0.7 ps pulses at a repetition rate of 463 MHz in a laser cavity with a fundamental frequency of 11.0 MHz ($z_c=18$ m). The third order RF spectrum at 1388 MHz is shown in Fig.4. The ratio of jitter to pulse separation is $3 \cdot 10^{-4}$. Further reduction of the cavity length did not result in an improvement of the time jitter, but at a rather short cavity length ($z_c = 8.6$ m) we found that the laser tended to operate at the same harmonic frequency of 139 MHz in a very broad range of pump power: the change of pump power level simply caused a change in the fraction of the non-soliton component without breaking-up the harmonic mode-locking.

2.2 Repetition rate self-stabilization in all-fibre soliton lasers

To understand the physical effects behind the complicated motion of pulses inside the laser cavity from the one hand and remarkably low time jitter from other hand let us look upon experimental facts and observations:

- regimes of tightly bunched pulses and harmonic mode-locking are equally stable and transition from one regime to another is initiated by alteration of the polarization controllers position;
- alteration of the polarization controller position results in a change of the laser gain and consequently the phase between the soliton and dispersive wave;
- in the spectral domain the main difference between the two regimes is in

intensity of the spectral side-bands, however it is impossible to say *a priori* whether a higher or lower intensity of non-soliton component corresponds to a certain regime:

- stable harmonic mode-locking has never been seen when the pulse spectrum was accompanied by multiple spectral side-bands;
- the slow motion in the transient regime corresponds to a normalized frequency difference between adjacent pulses of $\Omega \simeq 10^{-3}$;

Thus to analyze behaviour of solitons inside the laser cavity one needs to take into account a nonsoliton component generated by the propagating pulses. The soliton and the accompanying non-soliton component can be presented in the form of a fundamental soliton $\psi_s(t)$ and small perturbation $\delta\psi(t)$ i.e.

$$\psi(z, t) = \psi_s(z, t) + \delta\psi(t), \quad (1)$$

where

$$\psi_s(z, t) = \eta \text{sech}[\eta(t - \tau_s)] \exp i(\Omega_s t - \phi). \quad (2)$$

To consider the interaction between the solitons and non-soliton component we assume that in the steady state regime each soliton within a bunch comprising N pulses is accompanied by a non-soliton component, which being essentially a dispersive wave has an amplitude A and temporal width much longer than the soliton width. In other words a non-soliton component generated by a particular soliton is overlapping with several neighbouring solitons. To find analytically the result of the interaction between the

solitons and non-soliton components we also assume that (i) the initial time-separation between solitons is large enough to neglect the interaction between solitons, (ii) the time interval between adjacent solitons is approximately constant within the pulse bunch and (iii) all non-soliton components are broad enough so that each soliton interacts with all non-soliton components within the bunch. (Note that these assumptions do not affect basic conclusion in any significant way).

The perturbation for the n -th soliton $\delta\psi_n(t)$ within the bunch comprising N solitons can be written in the form:

$$\delta\psi_n(t) = A \exp(j\Omega t) \sum_{k=1}^{k=N} \exp[j((k-n)T\Omega + \phi_{k-n})] \quad (3)$$

where Ω is the frequency offset between the soliton and non-soliton component, ϕ_{i-j} is the phase difference between i -th soliton and a non-soliton component originated by the j -th soliton. Applying perturbation theory [26] we obtain

$$\begin{aligned} \delta\eta_n &= \text{Re} \int_{-\infty}^{+\infty} \psi_s(z, t) \delta\psi_n(t) dt = \\ & A\pi \text{sech} \frac{\pi(\Omega_s + \Omega)}{2} \sum_{k=1}^{k=N} \cos[(k-n)T\Omega + \phi_{k-n}], \end{aligned} \quad (4.a)$$

and

$$\begin{aligned} \delta\Omega_n &= \text{Im} \int_{-\infty}^{+\infty} \psi_s(t) \tanh(t) \delta\psi_n(t) dt = \\ & A\pi(\Omega + \Omega_s) \text{sech} \frac{\pi(\Omega_s + \Omega)}{2} \sum_{k=1}^{k=N} \cos[(k-n)T\Omega + \phi_{k-n}] \end{aligned} \quad (4.b)$$

In Eq.(4) ϕ_{k-n} is the phase difference between the k -th soliton and the dispersive wave from the n -th soliton. In the expression for $\delta\Omega_n$, ϕ_1 is the phase between the $(n-1)$ -th soliton and the n -th non-soliton component. From Eq.4.b one can find the relative frequency difference (or relative velocity) $\delta\Omega(n) = \delta\Omega_n - \delta\Omega_{n+1}$ of two adjacent solitons

$$\delta\Omega(n) = 2A\pi(\Omega + \Omega_s)\text{sech}\frac{\pi(\Omega + \Omega_s)}{2}\sin(\Phi - nT\Omega + \phi_+)\sin(\phi_- - \Phi) \quad (5)$$

where $\Phi = NT\Omega/2$, $\phi_{\pm} = (\phi_{-n} \pm \phi_{N-n})/2$.

The last expression clearly indicates the different velocity of individual solitons within the pulse bunch. Moreover the velocity difference between the adjacent pulses is not a constant across the bunch and depends on soliton position as well as on the phase difference between the solitons and non-soliton component ϕ_+ . To some extent the influence of the non-soliton component on the soliton behavior can be treated as a long-range soliton interaction, when parameters of a soliton changed not by an overlapping field of an adjacent soliton but by its non-soliton component. Eq.5 also suggests that the "long-range repulsion force" ($\delta\Omega > 0$) could be converted to "long-range attraction" ($\delta\Omega < 0$) provided an appropriate phase difference ϕ is set.

Thus to distribute tightly bunched pulses over the laser cavity one has to ensure $\delta\Omega(n) > 0$ for any n which can be done by a suitable adjustment of polarization controllers.

Typically the non-soliton component contains around 10% of the total energy and has a pulsewidth of about 500 ps [27]. From Eq.5 we can estimate

the velocity difference incurred by the non-soliton component as equal to 10^{-3} which agrees well with the experimentally observed picture.

When the solitons are nearly uniformly distributed along the laser cavity the electrostrictional effects become dominant not only because of weakening of the long range interaction force (due to less overlapping between a soliton and the adjacent non-soliton components) but also due to enhancement of the acoustically driven change of the refractive index. The theory of the refractive index change driven by electrostriction has been developed in a number of papers [28-30]. Briefly stated when a soliton propagates along an optical fibre the intense electric field generated in the fibre core distorts the fibre material and produce an acoustic wave. The acoustic wave causes density changes in the fibre which change the refractive index for the following pulses and imposes phase modulation. The acoustic wave travels radially outwards from the core and is reflected from the cladding boundary back towards the core. The round-trip time of the acoustic waves is ~ 20 ns. The refractive index change induced by a single soliton is very small and is about 10^{-11} corresponding to a normalized frequency shift of 10^{-5} which is much less than that induced by the non-soliton component.

However the cylindrical structure of the fibre can act as a resonator for acoustic waves excited at the appropriate natural eigenfrequencies of the fibre. The refractive index perturbation is thus considerably enhanced when the waves are periodically excited at these frequencies. The enhancement factor can be estimated from a simple model of a resonantly driven damped

harmonic oscillator and is of the order of τ_{ac}/T , where τ_{ac} is the damping constant of the oscillator and T is the resonant period. Since τ_{ac} and T are of the order of microseconds [29] and nanoseconds, respectively, the refractive index change is thus increased by a factor of 10^3 at resonant frequencies near 500 MHz.

Following methods developed in [28] we can obtain the expression for the refractive index change induced by an infinite pulse train

$$\delta n(t) = -\frac{\rho}{4cn^2} \left(\frac{\partial \epsilon}{\partial \rho} \right)^2 \frac{I_0 \tau_s}{\int F^2(r) dS} \times \sum_k \frac{B_k C_k}{\Omega_k} \exp(-\Gamma T) \frac{\sin(\Omega_k t) + \exp(-\Gamma T) \sin[\Omega_k(T-t)]}{1 + \exp(-2\Gamma T) - 2 \exp(-\Gamma T) \cos(\Omega_k T)} \quad (6)$$

where ρ is the fibre density, ϵ is the dielectric constant, Γ is the acoustic damping coefficient, I_0 is the pulse intensity, B_k, C_k are constants describing the overlap of acoustic, $F(r)$ is transverse field distribution and light fields and Ω_k is the k -th acoustic eigenfrequency. From Eq.6 one can see that whenever $\Omega_k T$ is close to 2π the denominator of the k -th term in the summation becomes small and the magnitude of refractive index perturbation increases. In this situation only one term dominates the summation and δn varies approximately sinusoidally.

Fig.5 plots the peak refractive index perturbation induced by a continuous stream of solitons as a function of repetition rate. The graph demonstrates that the peak perturbation has a complicated dependence on frequency and varies over almost 3 orders of magnitude with a peak value of $\sim 10^{-9}$. The reason for this behaviour is because resonances can occur not only at the

eigenfrequencies but also at frequencies Ω_r which satisfy to the condition $\Omega_r = m\Omega_n$, where m is an integer. Fig.6 shows the temporal variation of δn for the tenth acoustic frequency which is very close to sinusoidal. The pulses are situated under positive peaks of the curve. This imposes a phase modulation on the pulses which acts to stabilize the repetition rate.

Thus the theoretical consideration shows that the nonsoliton component plays a key role in the formation of stable pulse pattern. From the analysis we can suggest that the elimination by some means of the non-soliton component could result in better performance and easier repetition rate self-stabilization of fibre lasers. One possible way to achieve this it is the use of a MQW fast saturable absorber.

III. Soliton fibre laser with hybrid saturable absorber

III.1 Experimental configuration and results

The configuration of the laser is shown in Fig. 7. A NALM is formed between the output ports of a 60/40 coupler and includes ~ 100 metres of standard telecom fibre, a polarisation controller and a 2 metre long Er/Yb codoped fibre amplifier pumped by a miniature Nd:YAG source providing 200 mW of launched pump power at 1064 nm. An InGaAs/InP MQW saturable absorber and Bragg reflector stack is butted to the input port of the NALM. The MQW consists of 82 periods of 6.5 nm thick InP and 7.8 nm thick InGaAs. An isolator is spliced to the other port of the NALM to prevent feedback into the loop.

The laser has two regimes of operation. In the first regime, square pulses are generated at the fundamental cavity frequency of 1.8 MHz for almost any position of the polarisation controller. The duration of the pulses can be varied from ~ 10 ns down to ~ 500 ps by varying the pump power to the amplifier while the peak power of the pulses is fixed by the power required for switching in the NALM.

The second regime of operation is reached by adjusting the polarisation controller to set the correct phase bias in the NALM for soliton pulses to be generated. When the laser entered this regime of operation it was found that passive stabilization of the soliton repetition rate occurred with the repetition rate at harmonics of the fundamental frequency. Once the correct bias in the loop has been set the laser remains stable for several hours and after being switched off will self start in the passive harmonically modelocked regime. By using polarisation maintaining fibre in the loop it may be possible to fix the phase bias in the NALM and remove any need for polarisation control.

Output spectra for the soliton regime of operation taken at a repetition rate of 230 MHz are shown in Fig.8. Fig.8a shows a spectrum taken from the spare port on the WDM in the NALM. The spectral width is 1 nm indicating a pulsedwidth of 2.5 ps. The spectrum also demonstrates 20 dB suppression of the spectral sidebands commonly seen in fibre soliton lasers. This is attributable to the combined intensity discrimination of both the NALM and the saturable absorber. In the NALM the low intensity non soliton component which gives rise to the sidebands is switched out of the

laser. Any remaining non soliton radiation is then further suppressed by the action of the saturable absorber. Fig.8b shows a spectrum taken from the spare port of the NALM. This clearly shows that the soliton part of the spectrum has been switched back into the laser by the NALM while the non-soliton radiation is rejected from the laser cavity. (Note that the spectrum of non-soliton component agrees well with that calculated in [31] for the average soliton model).

A typical RF spectrum of the laser output intensity measured on a fast photodiode is shown in Fig.9. The main peak occurs at the pulse repetition rate while the smaller peaks are separated by the fundamental cavity frequency of 1.8 MHz. The spectrum demonstrates that adjacent modes of the laser are suppressed by over 40 dB and so once the laser is operating it is unlikely to switch between modes. The timing jitter of the pulses measured using RF spectra [25] is typically around 10 ps.

The presence of the NALM in the cavity fixes the peak power of the pulses to give the correct nonlinear phase difference required for switching of the pulses. In the soliton regime of operation this also fixes the pulsewidth and quantizes the energy of the pulse which allows the pulse repetition rate to be easily tuned by adjusting the pump power to the amplifier. By varying the pump power launched into the amplifier from the mini-YAG we were able to tune the pulse repetition rate in the range ~ 100 -400 MHz. To obtain higher repetition rates from the laser the mini-YAG was replaced by a high power YAG, and the length of standard telecom fibre with high dispersion was

replaced with ~ 30 m of dispersion-shifted fibre with zero dispersion around 1540 nm. An output from the laser cavity was provided by a 70/30 coupler just after the amplifier with 70% of the light being coupled of the cavity. The decrease of the cavity dispersion resulted in the pulsewidth reduce to less than 500 fs. Using this configuration we were able to achieve repetition rates of up to 2.085 GHz which corresponds to the 369th harmonic of the fundamental laser frequency of 5.6 MHz. The RF and optical spectra are shown in Figs.10 and 11 respectively. The optical spectrum shows strong suppression of the spectral sidebands.

III.2 MQW-structure as a passive phase modulator

The inclusion of the MQW saturable absorber into the laser cavity results in not only easier self-starting and cleanear pulses but also provides a passive phase modulation stabilizing the laser repetition rate.

To demonstrate this let us consider again a fibre laser with M pulses circulating inside the cavity with time interval T between them (for the sake of simplicity we assume that T is constant). For the saturable absorber we adopt a model of a three level system [32] as shown in Fig.12, where level 1 corresponds to the valence band and levels 2 and 3 are situated at the bottom and at upper states of the conductivity band. When pulses come through a MQW sample they excite free carriers to level 3 which then come down to level 2 with time constant τ_3 and then relax to the level 1 with time constant τ_2 . We can present the time dependence of the MQW refractive index in the form

$$n(t, T) = n_0 - N_2(t, T)\Delta n - N_3(t, T)\Delta n' \quad (7)$$

where n_0 is the undisturbed value of the refractive index, N_i are normalized density of free carriers (i.e. $N_1 + N_2 + N_3 = N_0 = 1$) and $\Delta n, \Delta n'$ are normalized refractive index coefficients for levels 2 and 3 respectively. The T -dependence of the free carrier density reflects the fact that the refractive index of the MQW depends on the laser repetition rate.

Assuming that the saturation intensity is significantly lower than the soliton intensity and that $\tau_2 \gg \tau_3 \approx \tau_0$ [32] we can conclude that the refractive index seen by any pulse from the laser is determined by the free carrier population at levels 2 and 3. (Note also that if free carrier lifetime of level 3 is much shorter than the pulsewidth then the refractive index of the MQW is independent of repetition rate). Thus to find the temporal dependence of refractive index one has to find population density dependence on the repetition rate. This can be done if we consider the following set of kinetic equations

$$\begin{aligned} N_1 &= N_0 - N_2 - N_3 \\ \frac{dN_2}{dt} &= -\frac{N_2}{\tau_2} + \frac{N_3}{\tau_3} \\ \frac{dN_3}{dt} &= -\frac{N_3}{\tau_3} \end{aligned} \quad (8)$$

When the laser operates in the harmonic regime the pulse stream incident on the absorber can be treated as infinitely long and population density can

be written as

$$N_2(t) = \sum_{k=0}^{\infty} \exp\left[-\frac{(t-kT)}{\tau_2}\right] [\Theta(t-kT) - \Theta(t-(k+1)T)] - \exp\left(-\frac{t}{\tau_3}\right) - [1 - \exp\left(-\frac{T}{\tau_2}\right)] \sum_{k=1}^{\infty} \exp\left[-\frac{(t-mT)}{\tau_3}\right] \Theta(t-kT) \quad (9.a)$$

$$N_3(t) = \exp\left(-\frac{t}{\tau_2}\right) + [1 - \exp\left(-\frac{T}{\tau_2}\right)] \sum_{m=1}^{\infty} \exp\left[-\frac{(t-mT)}{\tau_3}\right] \Theta(t-mT) \quad (9.b)$$

where $\Theta(t-mT)$ is the Heaviside function.

Thus each pulse coming through the saturable absorber sees the repetition rate dependent refractive index

$$\begin{aligned} n(T) &= n_0 - \Delta n \exp\left(-\frac{T}{\tau_2}\right) + (\Delta n - \Delta n') [1 - \exp\left(-\frac{T}{\tau_2}\right)] \exp\left(-\frac{T}{\tau_3}\right) \simeq \\ &\simeq n_0 - \Delta n \exp\left(-\frac{T}{\tau_2}\right) \end{aligned} \quad (10)$$

A time varying refractive index modulates the phase of the pulses and change the pulse carrier frequency by

$$\begin{aligned} \Delta\omega &= -\frac{z_a\omega_0}{c} \frac{dn}{dt} \Big|_{t=T} = -\frac{z_a\omega_0}{c} \left\{ \frac{\Delta n}{\tau_2} \exp\left(-\frac{T}{\tau_2}\right) + \right. \\ &\quad \left. + \frac{(\Delta n - \Delta n')}{\tau_3} [1 - \exp\left(-\frac{T}{\tau_2}\right)] \exp\left(-\frac{T}{\tau_3}\right) \right\} \approx \\ &\approx -\frac{z_a\omega_0}{c} \frac{\Delta n}{\tau_2} \exp\left(-\frac{T}{\tau_2}\right) \end{aligned} \quad (11)$$

where ω_0 is the carrier frequency, z_a is the thickness of the saturable absorber and c is the speed of the light. Eq.11 shows that $\Delta\omega < 0$ which decreases the group velocity of the pulses and provides a repulsive force between the pulses. In a harmonically mode-locked laser this keeps the pulses apart and stops

pulse bunches forming. The time dependence of $\Delta\omega$ means that a delayed pulse is slowed down less than a premature pulse which shows that the phase modulation provided by the saturable absorber is capable of retiming the pulses and stabilizing the repetition rate.

It is more intuitive to express the temporal variation of the refractive index in the more convenient form of a sinusoidally varying phase modulator. This suggests defining an effective modulation depth in terms of the saturable absorber parameters Δn and T/τ_2 to reflect the changes in strength of modulation with pulse spacing. Since we are approximating equation (7) by a sinusoidal function it is important that the first derivatives of the two functions are similar for $t \approx T$ where phase modulation of the pulses occurs so that the frequency shifts given by Eq.(11) are approximately the same. Considering the form of the first derivative of Eq.(11) we can present an expression in the form

$$\begin{aligned} n'(t) &= n_0 - \frac{\Delta n \exp(-T/\tau_2)}{2} [3 - \cos(\frac{2\pi t}{T})] = \\ &= n'_0 + \Delta n_{eff} \cos(\frac{2\pi t}{T}) \end{aligned} \quad (12)$$

where the definition of n'_0 ensures that $n(T) = n'(T)$. From the definition of Δn_{eff} it can be seen that for large values of T/τ_2 the strength of the modulation is small but increases as the ratio T/τ_2 decreases. This is demonstrated in Fig.13 where $n(t)$ and $n'(t)$ are plotted for comparison for the values $T/\tau_2=1$ and 2.5 with $n_0 = 3.0$ and $\Delta n_0=0.1$. For $T/\tau_2=0.5$ the effective modulation depth is $\Delta n_{eff}=0.02$ while for $T/\tau_2=2.5$ it is reduced to

$\Delta n_{eff}=0.004$ and it can be seen that in both cases the two curves are quite similar at the modulation peak justifying the approximations made above.

To measure lifetime of the carriers in our sample we performed a pump/probe experiment where the transmission of a weak pulse through a sample of the MQW was measured as a function of the time delay from an intensive probe pulse generated by the laser at frequency of 1.8 MHz. This yielded a lifetime for the absorption of the MQW of 15 ± 3 ns. (Note that we actually require the lifetime of the refractive index but since both processes depend upon the density of free carriers in the semiconductor the lifetime for the absorption and refractive index will be similar). The carrier lifetime is of the same order of magnitude as the soliton pulse spacing observed in the laser which further confirms that the MQW sample acts not only as a saturable absorber but also as a passive phase modulator.

IV. Time jitter in passively mode-locked fibre lasers

There are several sources of time jitter in mode-locked fibre lasers: pump power fluctuations, various thermal effects, and noise of the laser gain medium [33]. However a harmonically mode-locked fibre laser has an additional source of time jitter due to uncontrolled changes of adjacent pulse temporal positions and hence the jitter is significantly stronger than that which occurs in lasers operating at the fundamental frequency. In this sense a fibre soliton laser, operating in the harmonically mode-locked regime, is similar to a soliton transmission system: a soliton stream in a fibre laser

experiences periodic gain and loss and suffers from the same sources of time jitter such as the Gordon-Haus effect [34], soliton interaction with optical and acoustical fields. Extensive studies of soliton transmission systems which have been performed in the last several years [35-38] have revealed that in order to maintain the soliton stream intact over unlimited distances one has to incorporate into the transmission line spectral filtering and synchronous modulation. The existence of just one component (either filter or modulator) results only in a partial reduction of instability [36], while phase modulators have been shown to be able to suppress Gordon-Haus jitter with minimal generation of dispersive wave components [39]. In many cases the filtering action in passively mode-locked fibre lasers is provided by the laser gain medium while the modulation as we demonstrated above is achieved by slow perturbations of the laser cavity.

In order to estimate the time jitter of a passive harmonically mode-locked laser we consider the Nonlinear Schrödinger Equation (NSE). In the case of passively mode-locked fibre laser the NSE can be presented in the form

$$i\frac{\partial\psi}{\partial z} + \frac{1}{2}\frac{\partial^2\psi}{\partial\tau^2} + |\psi|^2\psi = iG\psi + i\beta\frac{\partial^2\psi}{\partial\tau^2} + (\phi_0 - \phi_2\tau^2)\psi + i\alpha|\psi|^2\psi + S(z), \quad (13)$$

where the left hand side is the unperturbed NSE while the first term on the right hand side describes the laser gain, the second stands for the intracavity laser filter, and the third term describes the action of the phase modulation. The fourth term represents modelocking by means of a fast saturable absorber, and $S(z)$ is the noise source from the laser amplifier. In the model

we have made an assumption that the time jitter is much less than the pulse period and therefore we consider T as a constant parameter.

Both self-induced modulators (acoustic and MQW) can be approximated by a sinusoidally driven phase modulator and corresponding parameters ϕ_i can be written in the form

$$\phi_0 = \begin{cases} k\delta n z_c & \text{for acoustic effect} \\ k\Delta n_{eff} z_a & \text{for MQW SA} \end{cases} \quad (14)$$

and $\phi_2 = \phi_0 \xi_c^2 / T^2$, where $\xi_c = z_c / z_d$ and z_c is the laser cavity length.

Applying perturbation theory for the NSE [23] and taking the solution of the unperturbed NSE in the form of Eq.(1) we obtain the equation for the soliton temporal position τ_s in the steady-state regime ($\eta \simeq 1$)

$$\frac{d^2 \tau_s(z)}{dz^2} + \frac{4\beta}{3} \frac{d\tau_s(z)}{dz} + 2\phi_2 \tau_s(z) = S_\Omega(z). \quad (15)$$

Here we assume that the noise impact on the soliton temporal position is driven by the soliton frequency fluctuations. The noise correlation function is [36]

$$\langle S_\Omega(z) S_\Omega^*(z') \rangle = \delta(z - z') \frac{(G^2 - 1)}{3N_0 \xi_c} = \delta(z - z') N_\Omega, \quad (16)$$

where $N_0 = W_s / h\nu$ is the number of photons per unit energy and W_s is the soliton energy.

Taking the Fourier transform of Eq.15 and solving the equation in the spatial frequency domain k we arrive at the expression for the rms time jitter ($z \rightarrow \infty$) σ_T

$$\sigma_T^2 = \int_{-\infty}^{+\infty} \langle |\tau_c(k)|^2 \rangle dk = \frac{3N_\Omega}{2\beta\phi_2} = \frac{(G^2 - 1)\Omega_f^2 T^2}{32N_0\phi_0\xi_c^2} \quad (17)$$

where $\beta = 2/(\Omega_f^2 \xi_c)$ and Ω_f is the dimensionless filter bandwidth.

In the ring laser described above we have $\phi_0 = 0.33$ rad, $\xi_c = 2.3$, $T = 3 \times 10^3$, $\Omega_f \approx 10$, $G^2 \approx 5$ and $N_0 = 3 \times 10^8$ which gives us $\sigma_T \approx 0.4$ or 160 fs in physical units in reasonably good agreement with the experimental results.

In the laser with the MQW SA based on standard telecom fibre and producing 2.5 ps pulses at 250 MHz we have $z_a = 1$ μm , $\tau_2 = 15$ ns, $\Delta n_{eff} = 0.04$, $T = 2500$, $\phi_0 = 0.17$ rad, and time jitter could be as low as 2.5 ps. Note also that using a saturable absorber with a shorter life-time should allow higher repetition rates to be achieved with subpicosecond time jitter.

V. Conclusion

The presented experimental results and theoretical consideration of passive harmonically mode-locked lasers indicate that the proper choice of components of a fibre laser could result in the design of a simple and reliable source of sub-picosecond pulses with repetition rate exceeding 1 GHz and time jitter between pulses below 10 ps.

The theoretical analysis indicates that periodic loss and gain experienced by the propagating pulses results in the formation of a non-soliton component which being essentially a dispersive wave affects the parameters of several neighbouring solitons. The effect of interactions between the solitons and accompanying non-soliton component is dominant and depending on the phase between nonlinear and dispersive waves the interaction force may at-

tract or repel adjacent solitons. In other words depending on the position of the polarization controllers one can get the regime of either tightly bunched pulses or pulses nearly uniformly distributed over the cavity.

Each pulse circulating inside the laser cavity emits a weak acoustic wave which affects the velocity of subsequent solitons via the electrostrictional effect. When the pulses are tightly bunched the acoustic effect is overshadowed by the action of the non-soliton component which dominates in this regime and is responsible for the complicated slow motion of pulses inside the laser cavity. However when the pulses become distributed quasi-uniformly over the laser cavity the influence of the non-soliton component diminishes while the acoustic effect is enhanced because the fibre acts as a low loss acoustic resonator. The enhanced acoustic effect then locks pulses at their temporal positions.

Despite the rather low time jitter observed in a ring configuration (below 1 ps) the polarization sensitivity of such lasers strongly restricts the possible range of applications of fibre soliton lasers. From this point of view a fibre laser with a hybrid saturable absorber looks more attractive since it offers better suppression of the non-soliton component with additional retiming action from the self-induced MQW phase modulator.

Finally note an important problem associated with the specific nature of harmonically mode-locked fibre soliton lasers. As was mentioned above pump power fluctuations do not affect the parameters of individual pulses but could result in a change of the number of circulating pulses. Thus in

the presence of pump power fluctuations the energy quantization effect may severely deteriorate time jitter characteristics of soliton fibre lasers. For example, the fundamental frequency of a laser with cavity length $\xi_c = 2$ and intracavity dispersion $k'' = 2 \cdot 10^{-28} \text{ s}^2/\text{cm}$ is around 2 MHz and therefore to maintain a low time jitter in a 10 GHz stream of solitons the pump power stability should be better than 10^{-4} . This may be difficult to achieve in practice but in the present laser configuration the stability could be improved by replacing the Nd:YAG laser with high power laser diodes.

References

1. I. N. Duling III, "Subpicosecond all-fibre erbium laser", *Electronics Letters*, **27**, 544-545, (1991)
2. D. J. Richardson, R. I. Laming, D. N. Payne, M. W. Phillips and V. J. Matsas, "320 fs soliton generation with passively mode-locked erbium fibre laser", *Electronics Letters*, **27**, 730-732, (1991)
3. M. Nakazawa, E. Yoshida, and Y. Kimura, "Low threshold, 290 fs erbium-doped fibre laser with a nonlinear amplifying loop mirror pumped by InGaAsP laser diodes", *Appl. Phys. Lett.* **59**, 2073-2075, (1991)
4. R. P. Davey, N. Langford, and A. I. Ferguson, "Interacting solitons in erbium fibre laser", *Electron. Lett.*, **27**, 1257-1259, (1991)
5. A. B. Grudinin, D. J. Richardson, and D. N. Payne, "Energy quantization in figure eight fibre laser", *Electron. Lett.*, **28**, 67-68, (1992)
6. V. J. Matsas, T. P. Newson, D. J. Richardson, and D. N. Payne, "Self-starting passively mode-locked fibre ring laser exploiting nonlinear polarization rotation", *Electron. Lett.*, **28**, 1391-1393, (1992)
7. V. J. Matsas, D. J. Richardson, T. P. Newson, and D. N. Payne, "Characterization of a self-starting, passively mode-locked fibre ring laser that exploits nonlinear polarization evolution", *Optics Lett.*, **18**, 358-360, (1993)
8. C. J. Chen, P. K. A. Wai, and C. R. Menyuk, "Soliton fibre ring laser", *Optics Lett.*, **17**, 417-419, (1992)
9. A. B. Grudinin, D. J. Richardson, and D. N. Payne, "Passive harmonic

mode-locking of a fibre soliton ring laser", *Electron. Lett.*, **29**, 1860-1861, (1993)

10. S. Gray, A. B. Grudinin, W. H. Loh, and D. N. Payne, "Femtosecond harmonically mode-locked fiber laser with time jitter below 1 ps", *Optics Lett.*, **20**, 189-191, (1995)

11. M. E. Fermann, M. J. Andrejco, M. L. Stock, Y. Silberberg, and A. M. Weiner, "Passive mode-locking in erbium fibre lasers with negative group delay", *Appl. Phys. Lett.*, **62**, 910-912, (1993)

12. V. J. Matsas, W. H. Loh, and D. J. Richardson, "Self-starting, passively mode-locked Fabry-Perot fibre soliton laser using nonlinear polarization evolution", *IEEE Photonics Tech. Lett.*, **5**, 492-494, (1993)

13. M. E. Fermann, K. Sugden, and I. Bennion, "Environmentally stable high-power soliton fibre lasers that use chirped fibre Bragg gratings", *Optics Lett.*, **20**, 1625-1627, (1995)

14. M. N. Islam, E. R. Sunderman, C. E. Soccolich, I. Bar-Joseph, N. Saurer, T. Y. Chang, and B. I. Miller, "Color center lasers passively mode-locked by quantum wells", *IEEE J. Quantum. Electron.*, **25**, 2454-2463, (1989)

15. M. Zirngibl, L. W. Stulz, J. Stone, J. Hugi, D. DiGiovanni, and P. B. Hansen, "1.2 ps pulses from passively mode-locked laser diode pumped Er-doped fibre ring laser", *Electron. Lett.*, **27**, 1734-1735, (1991)

16. U. Keller, W. H. Knox, and G. W. 'tHooft, "Ultrafast solid-state mode-locked lasers using resonant nonlinearities", *IEEE J. Quantum. Elec-*

tron., **28**, 2123-2133, (1992)

17. W. H. Loh, D. Atkinson, P. R. Morkel, M. Hopkinson, A. Rivers, A. J. Seeds, and D. N. Payne, "Passively mode-locked Er^{3+} fibre laser using a nonlinear mirror", Photonics Techn. Lett., **5**, 35-37, (1993)

18. K. V. Reddy, W. Riha, A. B. Grudinin, D. J. Richardson, J. E. Townsend, D. N. Payne, and M. N. Islam, "A turnkey 1.5 μ m picosecond Er/Yb fibre laser", Proc. OFC'93, Paper PD17, San-Jose, USA, 1993

19. K. Tamura, H. A. Haus, and E. P. Ippen, "Self-starting additive pulse mode-locked erbium fibre ring laser", Electron. Lett., **28**, 2226-2228, (1992)

20. K. Tamura, L. E. Nelson, H. A. Haus, and E. P. Ippen, "Soliton versus non-soliton operation of fibre ring lasers", Appl. Phys. Lett., **64**(2) 149-151, (1994)

21. K. Tamura, C. R. Doerr, L. E. Nelson, H. A. Haus, and E. P. Ippen, "Technique for obtaining high-energy ultrashort pulses from an additive-pulse mode-locked erbium-doped fibre ring laser", Optics Lett., **19**, 46-48, (1994)

22. E. Yoshida, Y. Kimura, and M. Nakazawa, "Laser diode-pumped femtosecond erbium-doped fibre laser with a sub-ring cavity for repetition rate control", Appl. Phys. Lett., **60**, 932-934, (1992)

23. M. L. Dennis, I. N. Duling III, "High repetition rate figure eight laser with extra-cavity feedback", Electron. Lett., **28**, 1894-1895, (1992)

24. I. Y. Khrushchev, D. J. Richardson, and E. M. Dianov, "Generation of 800 MHz stable train of subpicosecond solitons from the figure 8 laser",

European Conference on Optical Communications, Montreux, Switzerland, 1993, Paper MoC 2.2,

25. D. von der Linde, "Characterization of the noise in continuously operating mode-locked lasers", *Appl. Phys.*, **B 39**, 201, (1985)

26. A. Bondeson, M. Lisak, and D. Anderson, "Soliton perturbations: a variational principle for the soliton parameters", *Physica Scripta*, **20**, 479-485, (1979)

27. W. H. Loh, A. B. Gridinin, V. V. Afanasjev, and D. N. Payne, "Soliton interaction in the presence of a weak non-soliton component", *Optics Lett.*, **19**, 698-700, (1994)

28. E. M. Dianov, A. V. Luchnikov, A. N. Pilipetskii, and A. N. Starodumov, "Electrostrictional mechanism of soliton interaction on optical fibres", *Optics Lett.*, **15**, 314-316, (1990)

29. E. M. Dianov, A. V. Luchnikov, A. N. Pilipetskii, and A. N. Starodumov, "Long-range interaction of soliton pulse trains in a single-mode fibre", *Sov. Lightwave Commun.*, **1**, 37-45, (1991)

30. A. N. Pilipetskii, E. A. Golovchenko, and C. R. Menyuk, "Acoustic effect in passively mode-locked fibre ring lasers", *Optics Lett.*, **20**, 907-909, (1995)

31. N. J. Smith, K. J. Blow, and I. Andonovich, "Sideband generation through perturbations to the average soliton model", *J. Lightwave Techn.*, **10**, 1329-1333, (1992)

32. M. Wegener, I. Bar-Joseph, G. Sucha, M. N. Islam, N. Saurer,

T. Y. Chang, and D. Chelma, "Femtosecond dynamics of excitonic absorption in the infrared $\text{In}_x\text{Ga}_{1-x}\text{As}$ quantum wells", *Phys. Rev. B*, **39**, 12794-12801, (1989)

33. H. Haus, A. Mecozzi, "Noise in mode-locked lasers", *IEEE J. Quantum Electron.*, **29**, 983-996, (1993)

34. J. P. Gordon, H. A. Haus, "Random walk of coherently amplified solitons in optical fibre transmission", *Optics Lett.*, **11**, 665-667, (1986)

35. A. Mecozzi, J. D. Moores, H. A. Haus, and Y. Lai, "Soliton transmission control", *Optics Lett.*, **16**, 1841-1843, (1991)

36. A. Mecozzi, J. D. Moores, H. A. Haus, and Y. Lai, "Modulation and filtering control of soliton transmission", *J. Opt. Soc. Am. B*, **9**, 1350-1357, (1992)

37. M. Matsumoto and A. Hasegawa, "Numerical study of the reduction of instability in bandwidth-limited amplified soliton transmission", *Optics Lett.*, **18**, 897-899, (1993)

38. H. Kubota and M. Nakazawa, "Soliton transmission control in time and frequency domains", *IEEE J. Quantum Electron.*, **29**, 2189-2197, (1993)

39. N. J. Smith, K. J. Blow, W. J. Firth, and K. Smith, "Soliton dynamics in the presence of phase modulators", *Optics Commun*, **102**, 324-328, (1993)

Figure Captions

Fig.1 Experimental configuration of a passively mode-locked ring laser. WDM, wavelength division multiplexer; PC's, polarization controllers.

Fig.2 Typical optical spectrum from the passively mode-locked fibre laser

Fig.3 Time jitter as a function of repetition frequency for a total cavity length of 35 m

Fig.4 Third order RF spectrum for a repetition frequency of 463 MHz and cavity length of 18 m, indicating 600-fs (100-550 Hz) jitter

Fig.5 Peak refractive index perturbations in an optical fibre generated by a continuous stream of pulses

Fig.6 Acoustic response of an optical fibre to a pulse stream whose repetition rate of 463 MHz matches the 10th acoustic eigenfrequency. Resonant enhancement generates a peak refractive index change $\sim 10^{-9}$.

Fig.7 Experimental configuration of a passively mode-locked laser with hybrid saturable absorber.

Fig.8 Pulse spectrum of laser: (a) taken at the spare port of the WDM and indicating 20 dB suppression of the non-soliton component; (b) taken at the rejected port of the 60/40 coupler (this spectrum actually corresponds to the non-soliton component).

Fig.9 RF spectrum of the laser output intensity taken with resolution of 30 kHz.

Fig.10 RF spectrum of the 2 GHz passive harmonically mode-locked fem-

femtosecond soliton laser. Pump power fluctuations cause frequency hopping.

Fig.11 Optical spectrum of the 2 GHz femtosecond soliton laser.

Fig.12 The 3-level model of MQW-based passive phase modulator.

Fig.13 Illustration of the MQW refractive index changes using the simple model of equation (8) (solid lines) and the sinusoidal approximation defined by equation (12) (dotted lines) for (a) $T/\tau_2 = 1$ and $T/\tau_2 = 2.5$

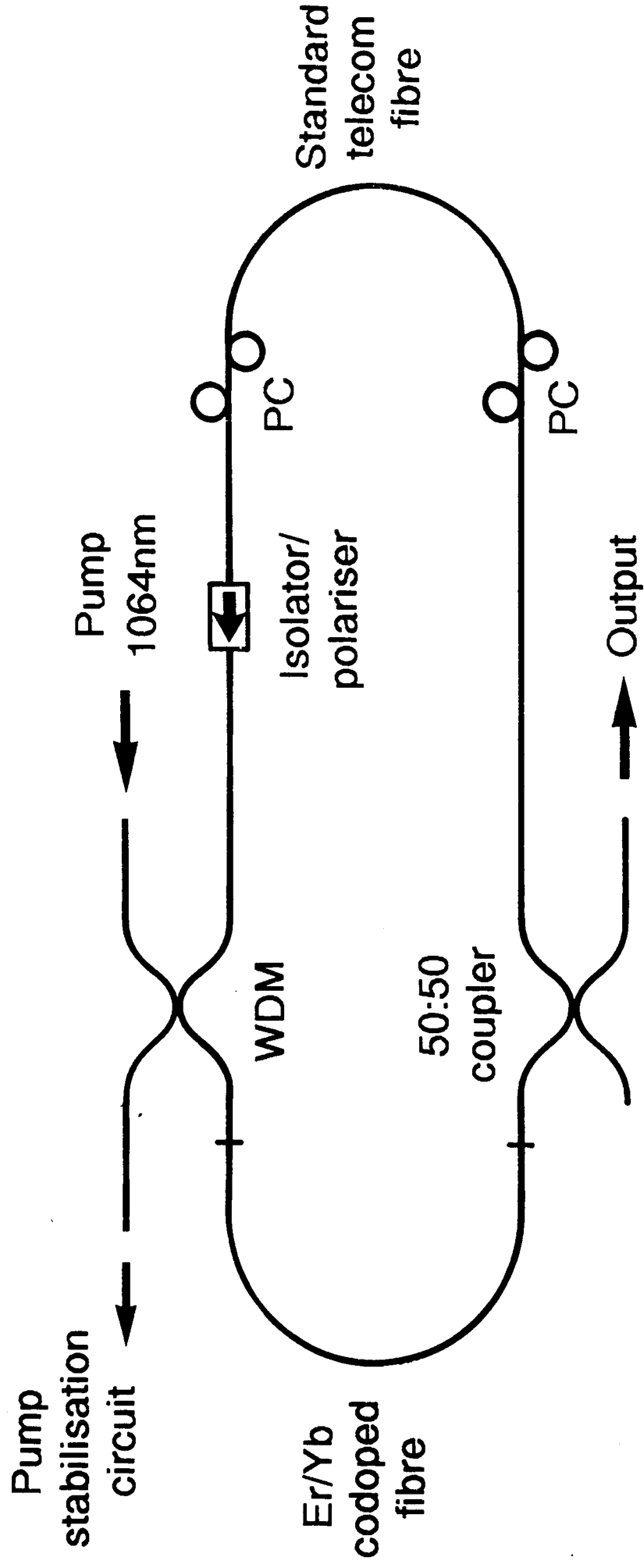


Fig 1

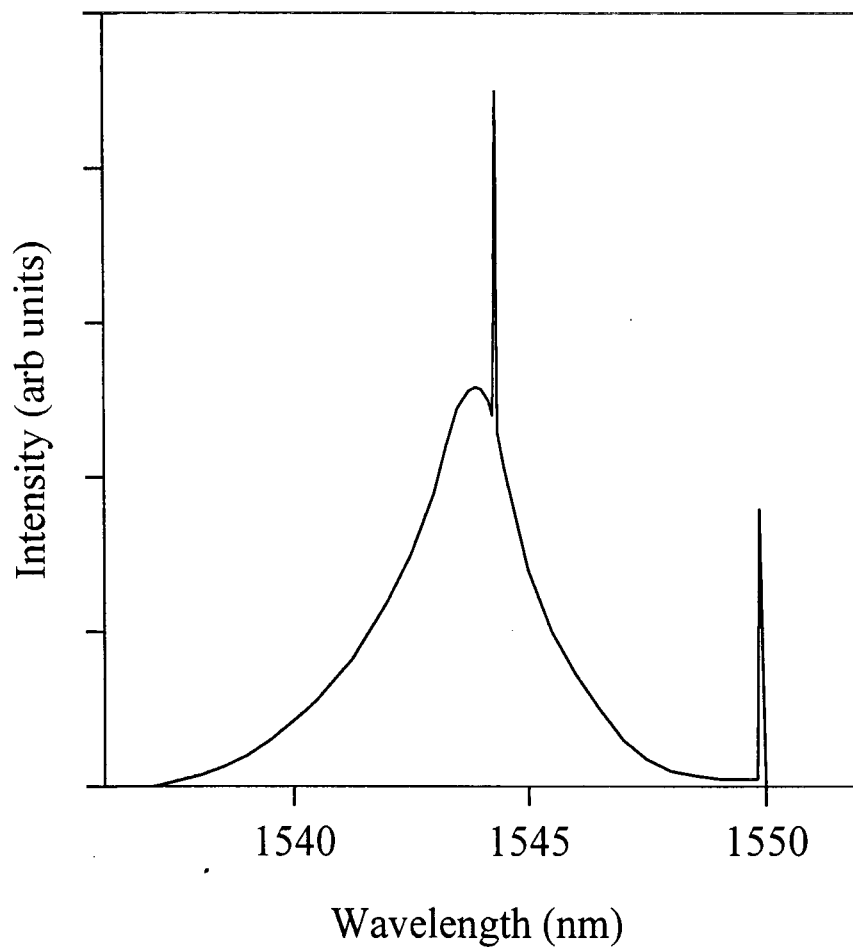


Fig 2

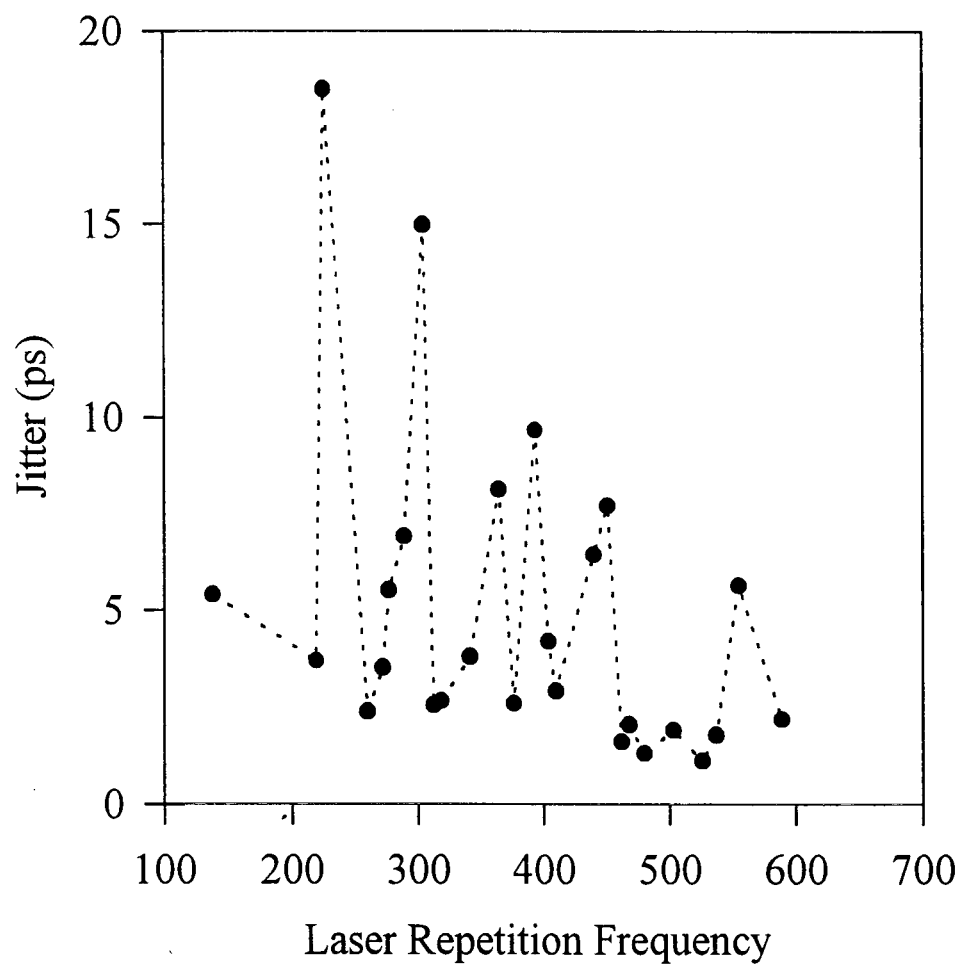


Fig 3

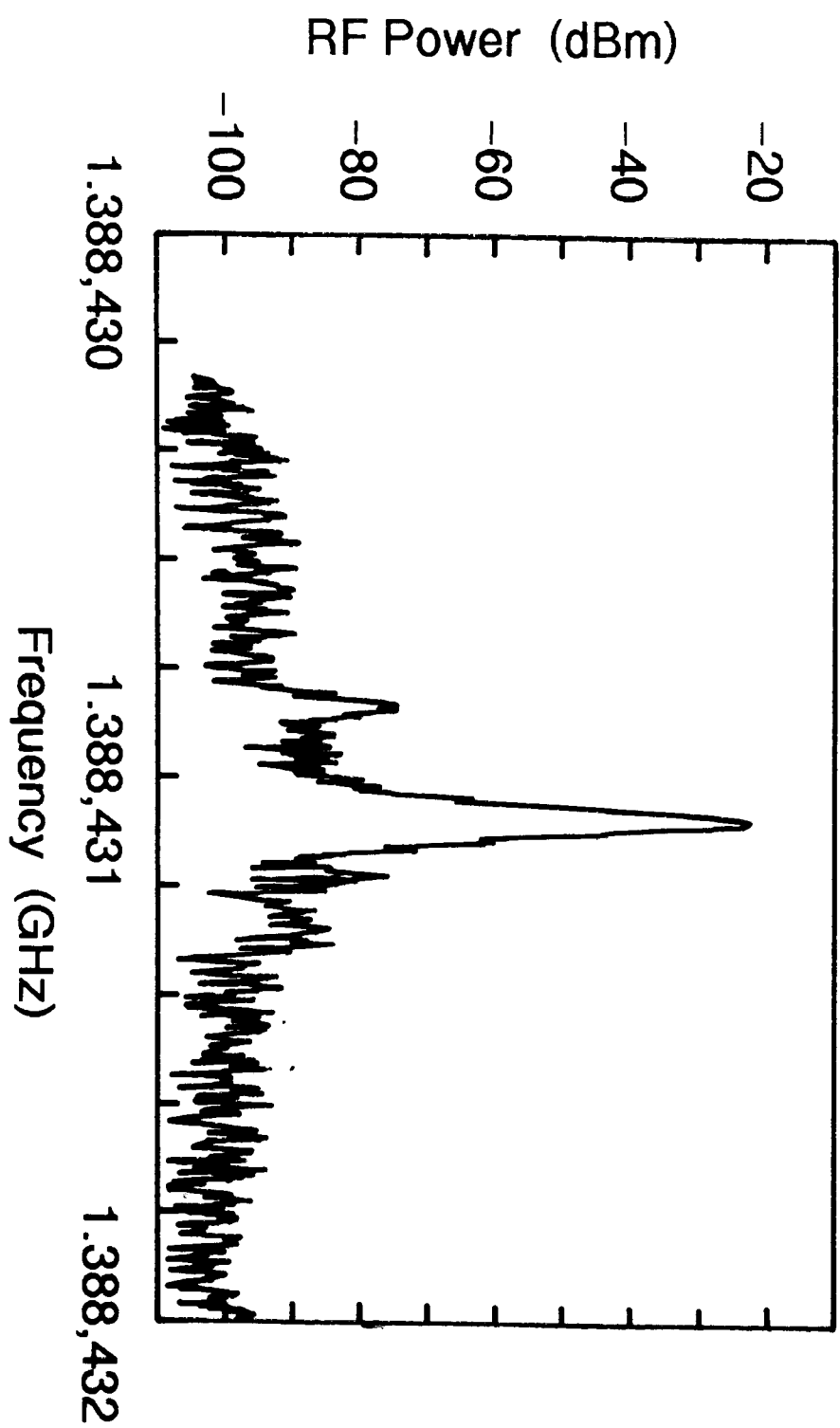


Fig 4

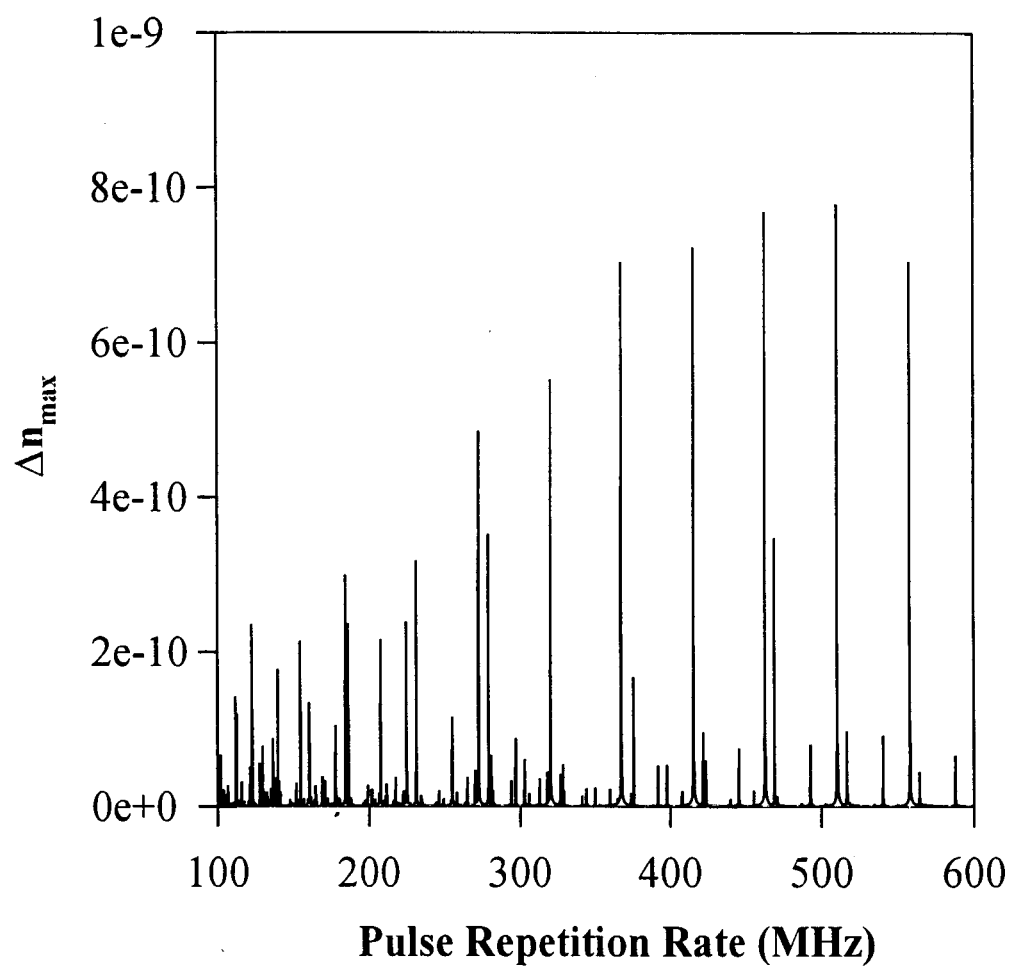


Fig 5

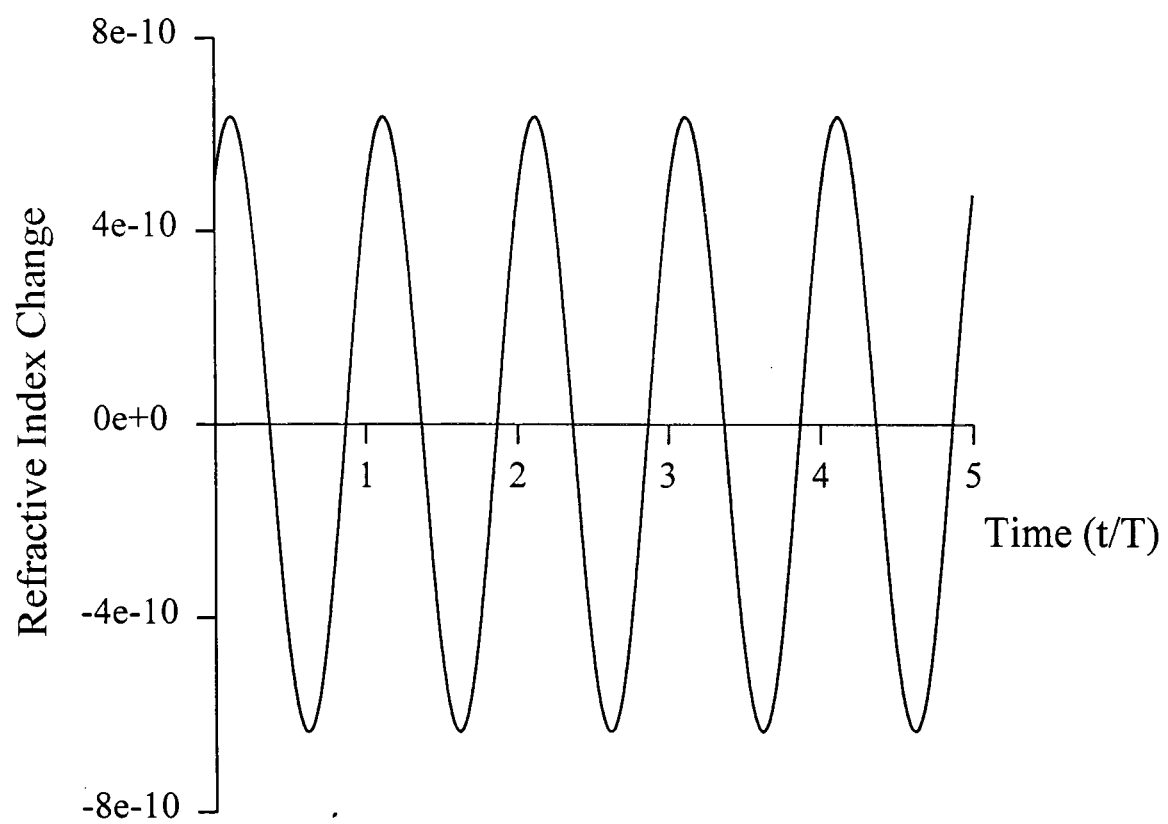


Fig 6

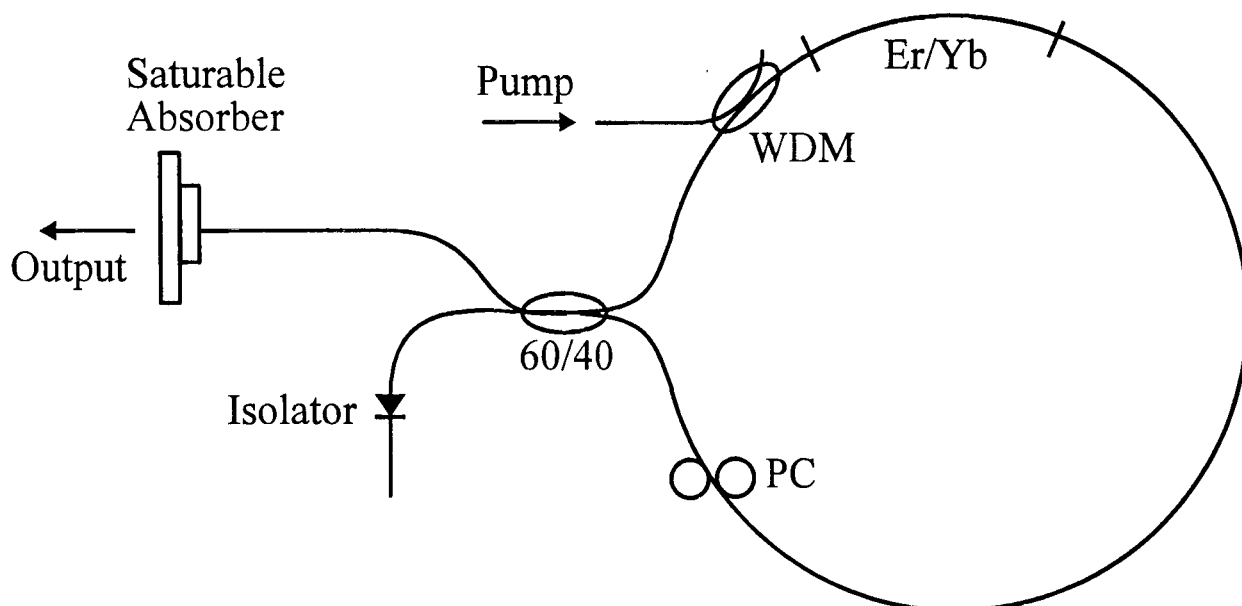


Fig 7

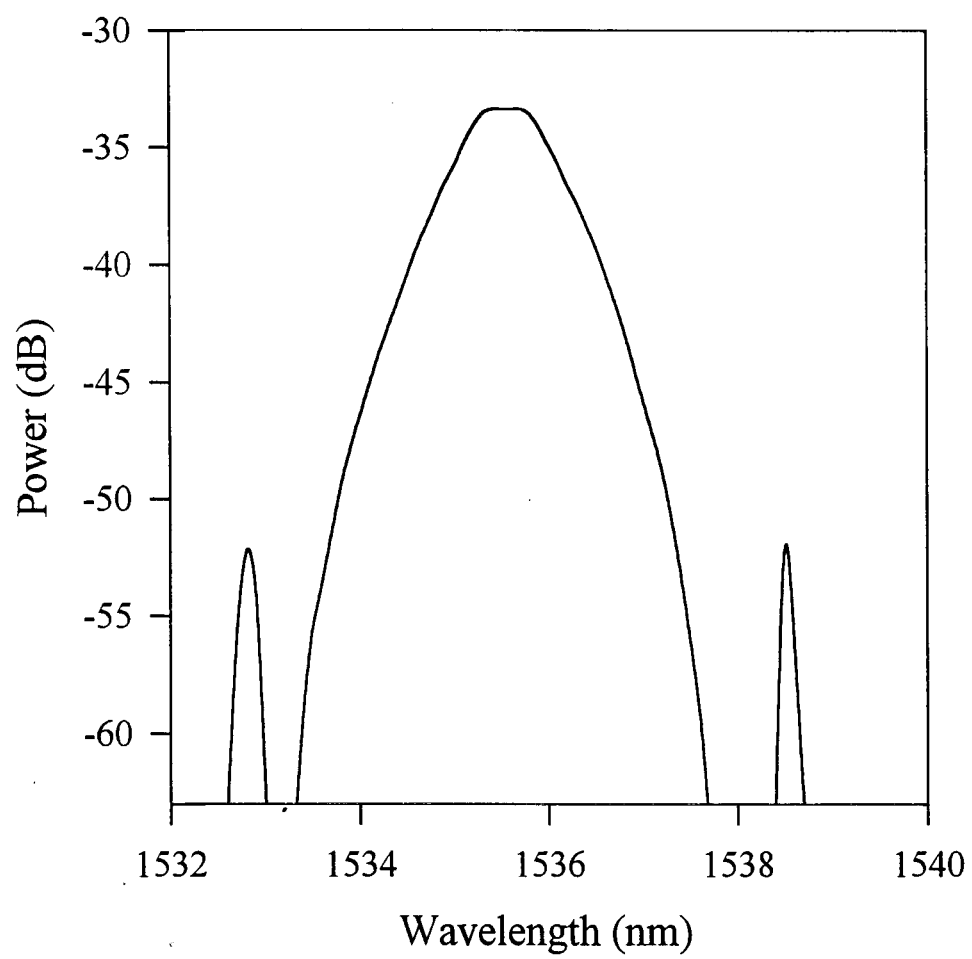


Fig 8 2

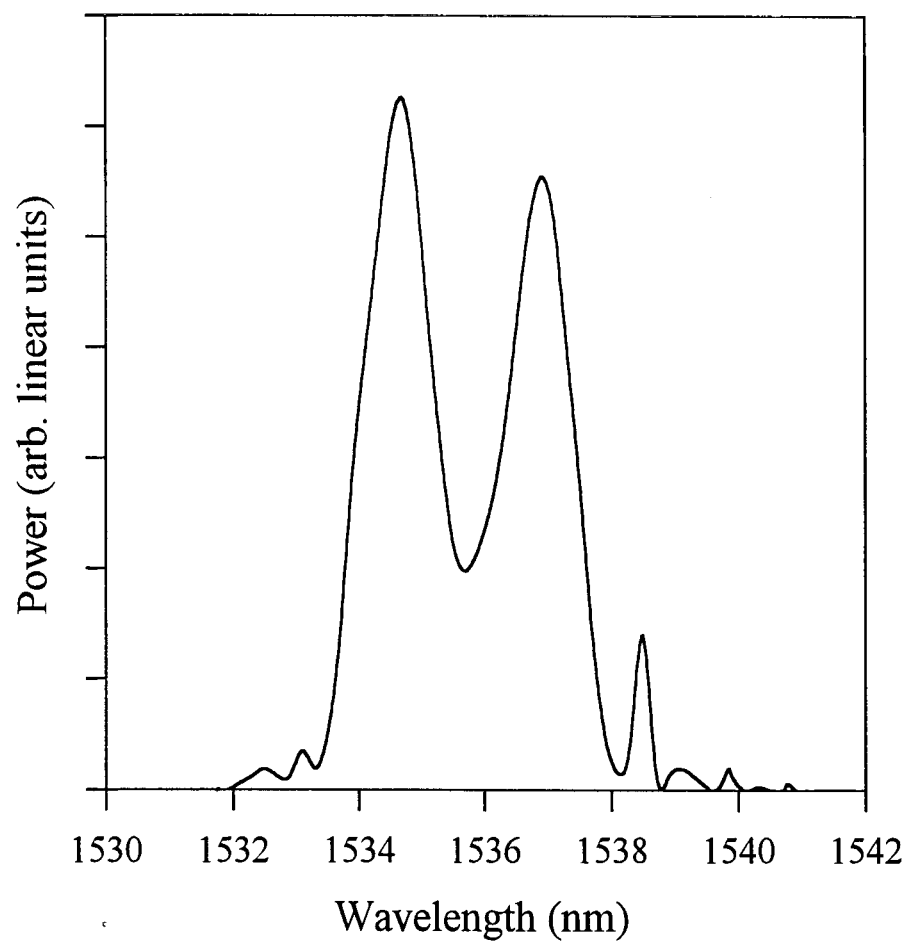


Fig 8^b

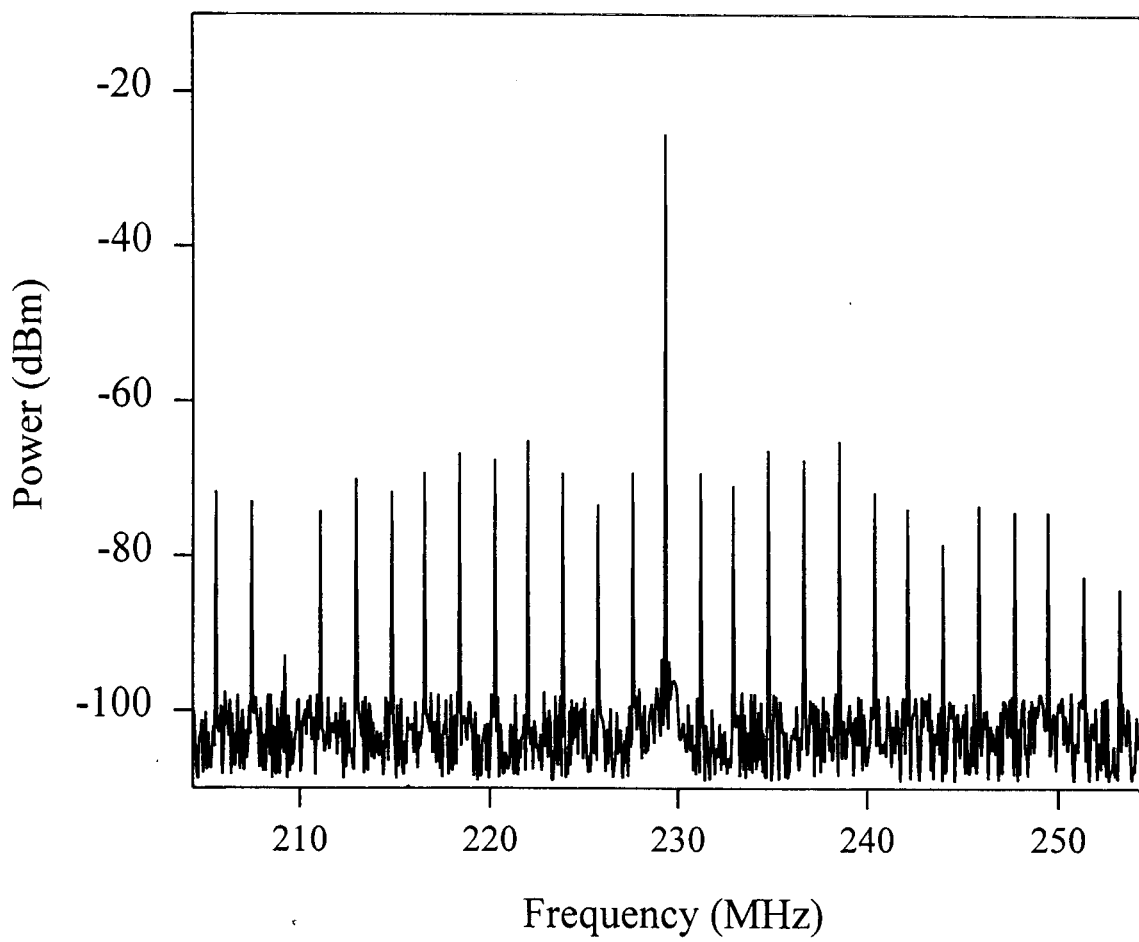


Fig 9

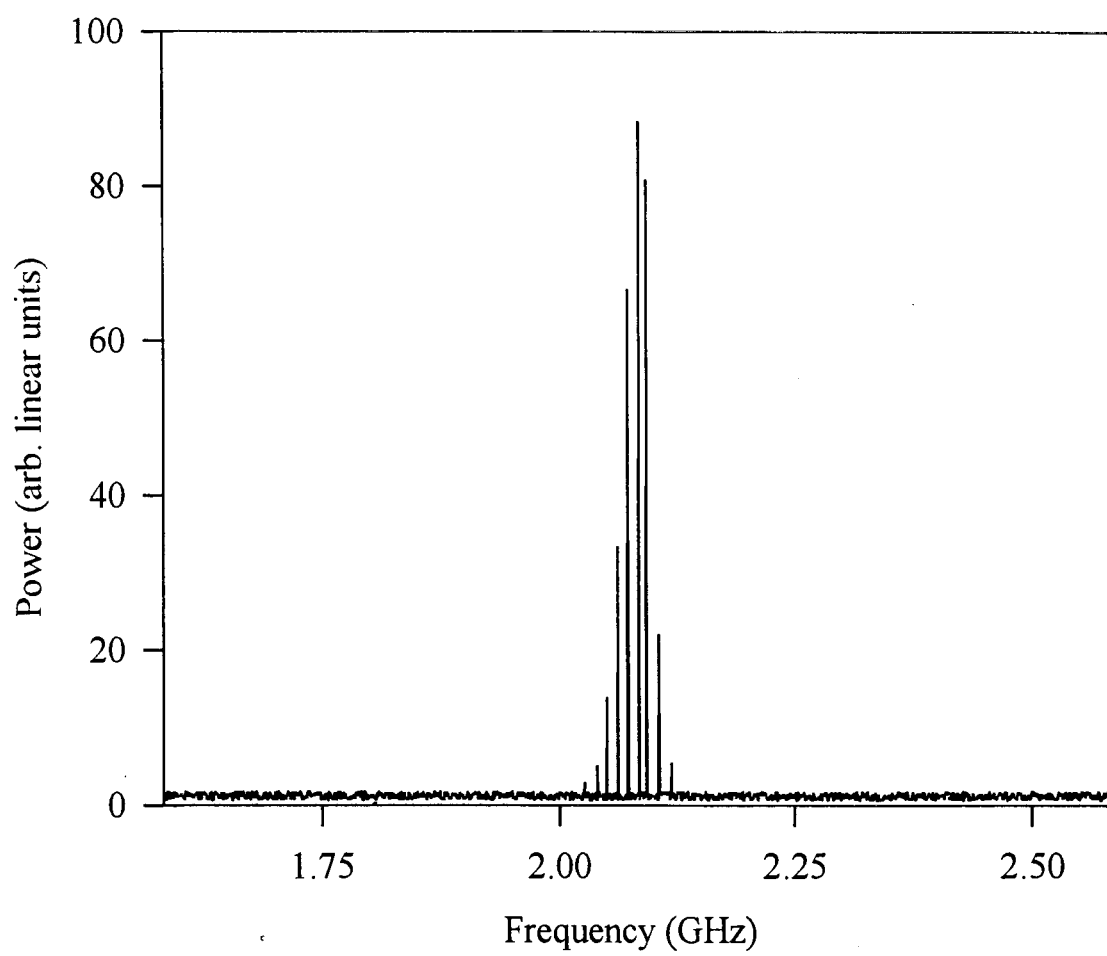


Fig 10

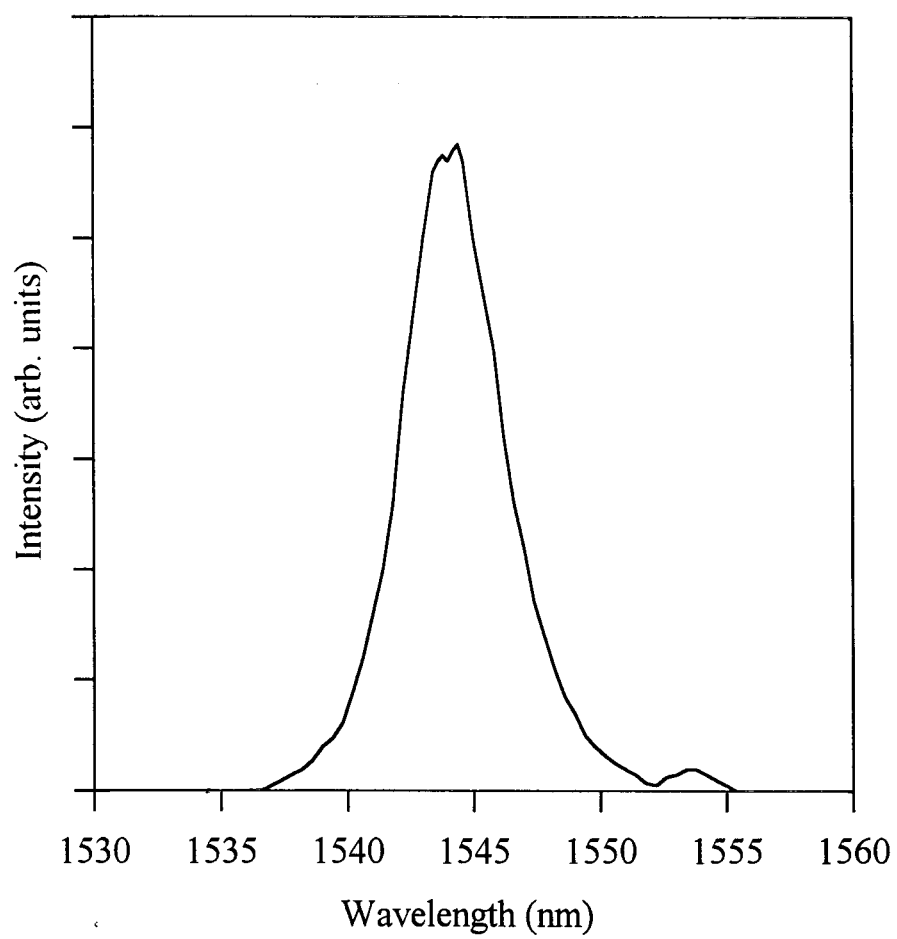


Fig 11

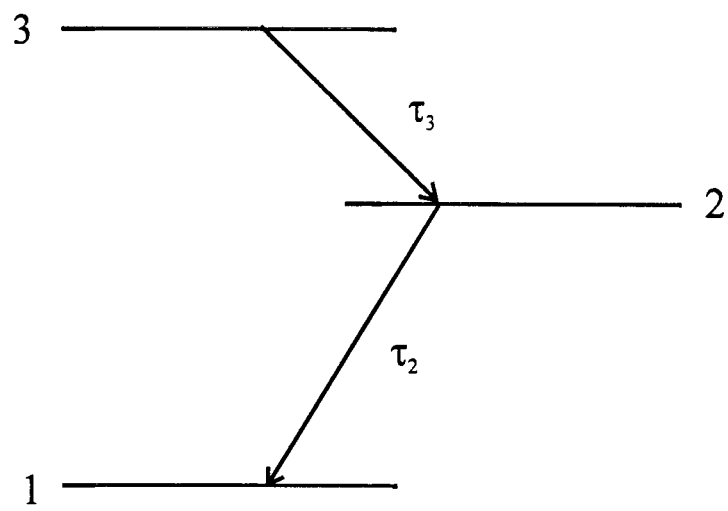


Fig 12

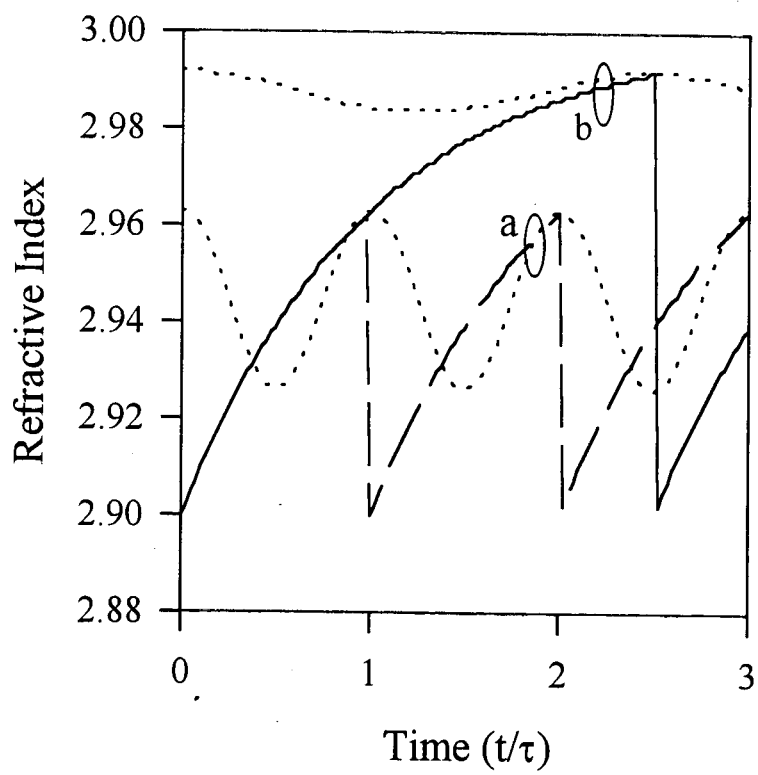


Fig 13